Analysis of the asymmetry factor in photophoresis problems with uniform polychromatic fields and spherical absorbers

L. A. Ambrosio[1,*], G. Gouesbet[2], J. Wang[3]

1: Department of Electrical and Computer Engineering. São Carlos School of Engineering, University of São Paulo. 400 Trabalhador são-carlense Ave. 13566-590, São Carlos, SP, Brazil
2: 2 CORIA-UMR 6614 - Normandie Université. CNRS-Université et INSA de Rouen. Campus Universitaire du Madrillet. 76800, Saint-Etienne du Rouvray, France
3: 3 School of Physics and Optoelectronic Engineering, Xidian University, 710071, Xi'an, China
*Corresponding author: leo@sc.usp.br

Keywords: Asymmetry factor, Photophoresis, Polychromatic light, Plane wave.

ABSTRACT

Photophoresis with plane waves and spherical absorbers is traditionally investigated by considering monochromatic radiation. The asymmetry factor, which is proportional to the photophoretic force, can be expressed in using the Mie theory in terms of an infinite sum of terms depending on the wavelength of the impinging light. Here, we analyze an extension of the photophoresis problem for a polychromatic uniform optical field. Such an analysis demands the introduction of a spectrum which describes the weight of each plane wave for the total, polychromatic field. We expect that this work can find applications or pave the way for more advanced investigations in diverse areas of physics and engineering such as optical levitation, optical trap displays and spectroscopy.

1. Introduction

In all that follows, the problem consists of an opaque, non-radiative, non-volatile, non-magnetic spherical absorber of size parameter $x = ka$ (a being its radius and $k = 2\pi/\lambda$ being the wave number, λ is the wavelength) immersed in a gaseous fluid. Relatively to the host medium, it has a refractive index $M = n_{sp} - im_{sp} = (\epsilon_{sp,r})^{1/2}$. From an optical point of view, the particle is therefore completely described in terms of a relative electric permittivity $\epsilon_{sp,r} = \epsilon_r' - i\epsilon_r''$. Notice that a time-dependence factor of the form $\exp(+i\omega t)$ is assumed, with ω being the angular frequency, and that for polychromatic fields all these parameters might be frequency-dependent.

In photophoresis by monochromatic plane waves and low Reynolds number, the asymmetry factor, which first appeared in a work by Yalamov et al. (Yalamov et al., 1976), embeds in itself all the electromagnetic part of the problem. Here, following the conventions presented in Ref. (Ambrosio et al., 2022) and considering a $+z$ propagating optical field, it shall be conveniently written in terms of the z component of the asymmetry vector $\mathbf{r}_{as}$ (Ambrosio et al., 2022):

$$r_{as,z} = \hat{\mathbf{z}} \cdot \mathbf{r}_{as} = \frac{\epsilon_r''}{2} I_\lambda \mathcal{I}_z, \tag{1}$$

where $I_\lambda = |E_0|^2/2\eta_m$ is the intensity of the wave, η_m is the intrinsic impedance of the medium and E_0 is the electric field strength. In Eq. (1), $\mathcal{I}_z$ is given in accordance with Eq. (17c) of Ref. (Ambrosio et al., 2022). In spherical coordinates (r, θ, ϕ):

$$\mathcal{I}_z = s\frac{x}{a} \int_0^{2\pi} \int_0^{\pi} \int_0^{a} B_z(r,\theta,\phi) r^3 \cos\theta \sin\theta dr d\theta d\phi, \tag{2}$$

with $B_z(r,\theta,\phi) = |\mathbf{E}_{int}(r,\theta,\phi)|^2/|E_0|^2$ being known as the dimensionless radiative intensity distribution function, source strength or normalized source function (Mackowski, 1989; Arnold et al., 1984; Greene et al., 1985). It must be emphasized that B_z is usually a fundamental parameter in photophoresis problems in the determination of the heat source function (the excitation term or inhomogeneous part of the heat transfer equation) $Q(r,\theta,\phi) = -(1/2)\,\mathrm{Re}[\nabla \cdot (\mathbf{E}_{int} \times \mathbf{H}_{int}^*)] = k\epsilon_r'' I_\lambda B_z(r,\theta,\phi)$ which is seen to be implicitly present in Eq. (1), since, from Eq. (2), $x/a = k$. Analytical solutions to Eq. (2) can be found, e.g., in Eq. (30b) of Ref. (Ambrosio et al., 2022) or, equivalently, in Eq. (8) of Ref. (Ambrosio, 2021), and read as:

$$\begin{aligned} \mathcal{I}_z \equiv \mathcal{I}_z(x,M,\omega) = & \frac{8\pi a^3}{|M|^2 x^3} \,\mathrm{Im} \sum_{n=1}^{\infty} \left\{ \frac{n(n+2)}{M} \left(c_n^* c_{n+1} R_{n+1} + |\eta_r|^2 d_n^* d_{n+1} R_n \right) \right. \\ & \left. - \left[\frac{n(n+2)}{n+1} \left(c_n c_{n+1}^* + |\eta_r|^2 d_n^* d_{n+1} \right) + \eta_r^* \frac{2n+1}{n(n+1)} c_n d_n^* \right] S_n \right\} \end{aligned} \tag{3}$$

In Eq. (3), c_n and d_n are the internal Mie coefficients and depend on the operating frequency, particle's geometry and electromagnetic properties (Gouesbet & Gréhan, 2017). Finally, η_r is the relative intrinsic impedance of the particle which, for a non-magnetic particle, can be written exclusively in terms of M, since $\eta_r = 1/\sqrt{\epsilon_{sp,r}} = 1/M$. Expressions for the quantities R_n and S_n can be found in Ref. (Mackowski, 1989), see Eqs. (59) and (61), with a correction for the sign in the latter, see for instance Eq. (14) and subsequent comments in Ref. (Ambrosio, 2020). For the convenience of the reader, they are here reproduced:

$$R_n = \frac{\mathrm{Im}\left[M\psi_{n+1})Mx)\psi_n^*(Mx)\right]}{\mathrm{Im}[M^2]} \tag{4}$$

and

$$\begin{aligned} S_n = -\frac{i}{2\,\mathrm{Im}[M^2]} \Bigg\{ & x\left(M|\psi_n(Mx)|^2 + M^*|\psi_{n+1}(Mx)|^2 \right) \\ & - \left(M + 2(n+1)\frac{\mathrm{Re}[M^2]}{M} \right) R_n + (2n+1) M^* R_{n+1} \Bigg\} \end{aligned} \tag{5}$$

where $\psi_n(z)$ is a Ricatti-Bessel function Gouesbet & Gréhan (2017).

The electric field $\mathbf{E}_{int}$ inside the sphere is given in accordance with the Mie theory. Explicitly introducing the ω-dependence, they can be written as:

$$E_{int,r} \equiv E_{int,r}(\mathbf{r},\omega) = \sum_{n=1}^{\infty} E_0(\omega)(-i)^{n+1}(2n+1)c_n(\omega)\frac{\psi_n[k_{sp}(\omega)r]}{[k_{sp}(\omega)r]^2}P_n^1(\cos\theta)\cos\phi, \tag{6}$$

$$\begin{aligned} E_{int,\theta} \equiv E_{int,\theta}(\mathbf{r},\omega) = \sum_{n=1}^{\infty} E_0(\omega)(-i)^{n+1}E_n \Bigg[& c_n(\omega)\frac{\psi_n'[k_{sp}(\omega)r]}{k_{sp}(\omega)r}\tau_n^1(\cos\theta) \\ & - i\frac{k(\omega)}{k_{sp}(\omega)}d_n(\omega)\frac{\psi_n[k_{sp}(\omega)r]}{k_{sp}(\omega)r}\pi_n^1(\cos\theta)\Bigg]\cos\phi, \end{aligned} \tag{7}$$

$$\begin{aligned} E_{int,\phi} \equiv E_{int,\phi}(\mathbf{r},\omega) = & i\sum_{n=1}^{\infty} E_0(\omega)(-i)^{n+1}E_n \Bigg[ic_n(\omega)\frac{\psi_n'[k_{sp}(\omega)r]}{k_{sp}(\omega)r}\pi_n^1(\cos\theta) \\ & + \frac{k(\omega)}{k_{sp}(\omega)}d_n(\omega)\frac{\psi_n[k_{sp}(\omega)r]}{k_{sp}(\omega)r}\tau_n^1(\cos\theta)\Bigg]\sin\phi. \end{aligned} \tag{8}$$

In Eqs. (6)-(8), $E_n = (2n+1)/[n(n+1)]$, $k_{sp} = Mk$ is the wave number in the particle, $P_n^1(\cos\theta)$ is an associated Legendre polynomial, and $\pi_n^1(\cos\theta) = P_n^1(\cos\theta)/\sin\theta$ and $\tau_n^1(\cos\theta) = dP_n^1(\cos\theta)/d\theta$ are generalized Legendre functions Gouesbet & Gréhan (2017). Once Eqs. (6)-(8) are replaced in Eq. (2), the asymmetry factor assumes the form provided by Mackowski in Ref. (Mackowski, 1989) under the time harmonic convention $\exp(-i\omega t)$ or, alternatively, Eq. (8) of Ref. (Ambrosio, 2021) for $\exp(+i\omega t)$, with the coefficients g_n in this equation set equal to 1, in accordance with Eq. (3) above.

2. Extension to the polychromatic incidence

Let us now extend the previous analysis to polychromatic uniform fields constructed from superpositions of plane waves. To do so, remember that the instantaneous phasor form for the fields in Eqs. (6)-(8) is $\mathbf{E}_{int}\exp(+i\omega t)$ and let us consider a polychromatic field of the form

$$\mathbf{X}_{int}(\mathbf{r},t) = \int_{-\infty}^{\infty} \mathbf{X}_{int}(\mathbf{r},\omega)e^{+i\omega t}d\omega, \tag{9}$$

with the inverse relation

$$\mathbf{X}_{int}(\mathbf{r},\omega) = \frac{1}{2\pi}\int_{-\infty}^{\infty} \mathbf{X}_{int}(\mathbf{r},t)e^{-i\omega t}dt, \tag{10}$$

In Eqs. (9) and (10), $\mathbf{X} = \mathbf{E}$ or $\mathbf{H}$. As a particular case of Eqs. (9) and (10), for an optical field composed of red, green and blue plane waves (say, with $\lambda = 632.8$, 543.5 and 441.6 nm, respectively):

$$\mathbf{E}_0(\omega) = \sum_{j=1}^{3} \mathbf{E}_0(\omega_j)\delta(\omega - \omega_j), \tag{11}$$

with $\mathbf{E}_0(\omega_j)$ corresponding to the electric field strength of the j-th plane wave. In Eq. (11), $\delta(.)$ is the Dirac delta function. Finally, Eq. (9) is further reduced for the instantaneous phasor form of a plane wave at a fixed angular frequency ω_0 by setting $\mathbf{E}_0(\omega) = E_0\delta(\omega - \omega_0)$.

The effect of Eqs. (9) and (10) on the heat source function can be quantified as follows. First, we evaluate $\mathbf{E}_{int} \times \mathbf{H}^*_{int}$:

$$\begin{aligned} \mathbf{E}_{int} \times \mathbf{H}^*_{int} &= \int_{-\infty}^{\infty} \mathbf{E}_{int}(\mathbf{r},\omega)e^{i\omega t}d\omega \times \int_{-\infty}^{\infty} \mathbf{H}^*_{int}(\mathbf{r},\omega')e^{-i\omega' t}d\omega' \\ &= \int_{-\infty}^{\infty}\int_{-\infty}^{\infty} \mathbf{E}_{int}(\mathbf{r},\omega) \times \mathbf{H}^*_{int}(\mathbf{r},\omega')e^{i(\omega-\omega')t}d\omega d\omega' \end{aligned} \tag{12}$$

Equation (12) is averaged over time using the fact that:

$$\lim_{T\to\infty} \frac{1}{T} \int_{-T/2}^{T/2} e^{i(\omega-\omega')t}dt = \begin{cases} 1, & \omega = \omega' \\ 0, & \text{otherwise} \end{cases} \tag{13}$$

thus leading to

$$\langle \mathbf{E}_{int}(\mathbf{r},t) \times \mathbf{H}^*_{int}(\mathbf{r},t)\rangle = \int_{-\infty}^{\infty} \mathbf{E}_{int}(\mathbf{r},\omega) \times \mathbf{H}_{int}(\mathbf{r},\omega)d\omega. \tag{14}$$

From Eqs. (12)-(14), the heat source function then becomes

$$\begin{aligned} Q &= -\frac{1}{2}\,\mathrm{Re}\left[\nabla \cdot \langle \mathbf{E}_{int}(\mathbf{r},t) \times \mathbf{H}^*_{int}(\mathbf{r},t)\rangle\right] = -\frac{1}{2}\,\mathrm{Re}\left[\nabla \cdot \left(\int_{-\infty}^{\infty} \mathbf{E}_{int}(\mathbf{r},\omega) \times \mathbf{H}^*_{int}(\mathbf{r},\omega)d\omega\right)\right] \\ &= -\frac{1}{2}\,\mathrm{Re}\left[\int_{-\infty}^{\infty} \nabla \cdot \left(\mathbf{E}_{int}(\mathbf{r},\omega) \times \mathbf{H}^*_{int}(\mathbf{r},\omega)\right) d\omega\right] = \int_{-\infty}^{\infty} \frac{1}{2}\omega\epsilon_m\epsilon''_r(\omega)|\mathbf{E}_{int}(\mathbf{r},\omega)|^2 d\omega \\ &= \int_{-\infty}^{\infty} Q(\mathbf{r},\omega)d\omega \end{aligned} \tag{15}$$

For the multichromatic case given in Eq. (11), Eq. (12) becomes:

$$\begin{aligned}\mathbf{E}_{int} \times \mathbf{H}^*_{int} &= \sum_{j=1}^{3} \mathbf{E}_{int}(\mathbf{r}, \omega_j) e^{i\omega_j t} \times \sum_{p=1}^{3} \mathbf{H}_{int}(\mathbf{r}, \omega_j) e^{-i\omega_p t} \\ &= \sum_{j=1}^{3} \sum_{p=1}^{3} \mathbf{E}_{int}(\mathbf{r}, \omega_j) \times \mathbf{H}_{int}(\mathbf{r}, \omega_j) e^{i(\omega_j - \omega_p)t}.\end{aligned} \tag{16}$$

Equation (16) is again averaged over time. Instead of Eq. (13), one now uses the fact that:

$$\lim_{T\to\infty} \frac{1}{T} \int_{-T/2}^{T/2} e^{i(\omega_j - \omega_p)t} dt = \delta_{\omega_j, \omega_p}, \tag{17}$$

where δ_{ij} is the Kronecker delta. This leads to

$$\langle \mathbf{E}_{int}(\mathbf{r}, t) \times \mathbf{H}^*_{int}(\mathbf{r}, t) \rangle = \sum_{j=1}^{3} \mathbf{E}_{int}(\mathbf{r}, \omega_j) \times \mathbf{H}_{int}(\mathbf{r}, \omega_j) \tag{18}$$

Similarly, from Eqs. (16)-(18) the following expression is found for the heat source function:

$$\begin{aligned}Q &= -\frac{1}{2} \operatorname{Re} \left[\nabla \cdot \left(\sum_{j=1}^{3} \mathbf{E}_{int}(\mathbf{r}, \omega_j) \times \mathbf{H}^*_{int}(\mathbf{r}, \omega_j) \right) \right] = \sum_{j=1}^{3} \frac{1}{2} \omega_j \epsilon_m \epsilon''_r(\omega_j) |\mathbf{E}_{int}(\mathbf{r}, \omega_j)|^2 \\ &= \sum_{j=1}^{3} Q(\mathbf{r}, \omega_j)\end{aligned} \tag{19}$$

It is then seen that Eq. (15) implies on $\mathcal{I}_z$ assuming the form

$$\mathcal{I}_z = \int_{-\infty}^{\infty} \mathcal{I}_z(x, M, \omega) d\omega, \tag{20}$$

while Eq. (19) leads to

$$\mathcal{I}_z = \sum_{j=1}^{3} \mathcal{I}_z(x, M, \omega_j). \tag{21}$$

In Eqs. (20) and (21), the integrand and the terms in the summation are calculated through Eq. (3) for an arbitrary frequency ω or for a discrete set of frequencies ω_j. Notice further that it is only possible to derive Eqs. (20) and (21) through a time-averaging process of the optical fields, since such a process allows one to rule out the interference terms observed in Eqs. (12) and (16). The same process reveals that $r_{as,z}$ in Eq. (1) assumes the same form of Eqs. (20) and (21).

3. Examples

As a first example of calculation of $r_{as,z}$, let us consider Eq. (21) and assume a polystyrene sphere whose real and imaginary parts of its refractive index with respect to air will be assumed to take values retrieved from Fig. 2 of Ref. (Velazco-Roa & Thennadil, 2007). The host medium is air ($\eta_m \approx$ 377 Ω), and three wavelengths of $\lambda_1 = 450$ nm, $\lambda_2 = 700$ nm and $\lambda_3 = 950$ nm are considered for the calculations. The field strengths are normalized, such that $E_0(\omega_j) = 1, \forall j$.

From the data presented for the Mie curves in Fig. 2 of Ref. (Velazco-Roa & Thennadil, 2007), one finds approximate values of $M_1 = 1.640 - i2.205 \times 10^{-3}$, $M_2 = 1.588 - i3.453 \times 10^{-3}$ and $M_3 = 1.564 - i4.224 \times 10^{-3}$ for the wavelengths λ_1, λ_2 and λ_3, respectively. This means that such particles are weak absorbers. Figure 1 shows $r_{as,z}$ as a function of the radius of the particle (20 nm $\leq a \leq$ 2 μm) for each wavelength, together with the total $r_{as,z}$. For the entire range of a, it is seen that $r_{as,z} > 0$, which corresponds to a negative photophoretic force. Notice that the total $r_{as,z}$ mimics the behavior of the individual curves, whose overall behavior are quite similar.

As a second example, we now assume a gold plasmonic particle. Such a spherical scatterer is highly absorbent, and its refractive index changes significantly over the range of optical frequencies [10]. For instance, according to data retrieved from Ref. (Magnozzi et al., 2018) (see also data available at https://refractiveindex.info/?shelf=main &book=Au&page=Magnozzi-25C) and for the same wavelengths as before, $M_1 = 1.4783 - i1.86$, $M_2 = 0.12309 - i4.1567$ and $M_3 = 0.16524 - i6.2423$. Figure 2 reveals the behavior of $r_{as,z}$ for the same radii as before. In contrast with Fig. 1, $r_{as,z} < 0$, which corresponds to a positive photophoretic force.

As a final example, in Fig. 3 we see the expected $r_{as,z}$ as a function of a for Gallium arsenide (Papatryfonos et al., 2021), which is a fundamental material in optoelectronics (see also data available at https://refractiveindex.info/?shelf=main&book=GaAs&page=Papatryfonos). Here, $\lambda_1 = 500$ nm, $\lambda_2 = 700$ nm and $\lambda_3 = 900$ nm, for which $M_1 = 4.2230 - i0.45325$, $M_2 = 3.7223 - i0.12964$ and $M_3 = 3.5325 - i1.9044 \times 10^{-4}$. In Fig. 3(a) we have weighted the field strengths such that $E_0(\omega_1) = E_0(\omega_2) = E_0(\omega_3) = 1$, while in Fig. 3(b) we have set $E_0(\omega_1) = E_0(\omega_2) = E_0(\omega_3)/1000 = 1$. It becomes clear that the total value of $r_{as,z}$ shifts from positive to negative by simply considering different field strengths. Therefore, in the more general case where $E_0(\omega)$ represents a spectrum over, say, the visible or any other range, the overall behavior for the asymmetry factor can be quite distinguished from that arising from a monochromatic incidence.

4. conclusion

In this work we have presented, for the first time to the best of the authors' knowledge, an approach to investigate photophoresis with polychromatic uniform light. The theoretical analysis indicates that the asymmetry factor, after a time averaging process, can be simply written as

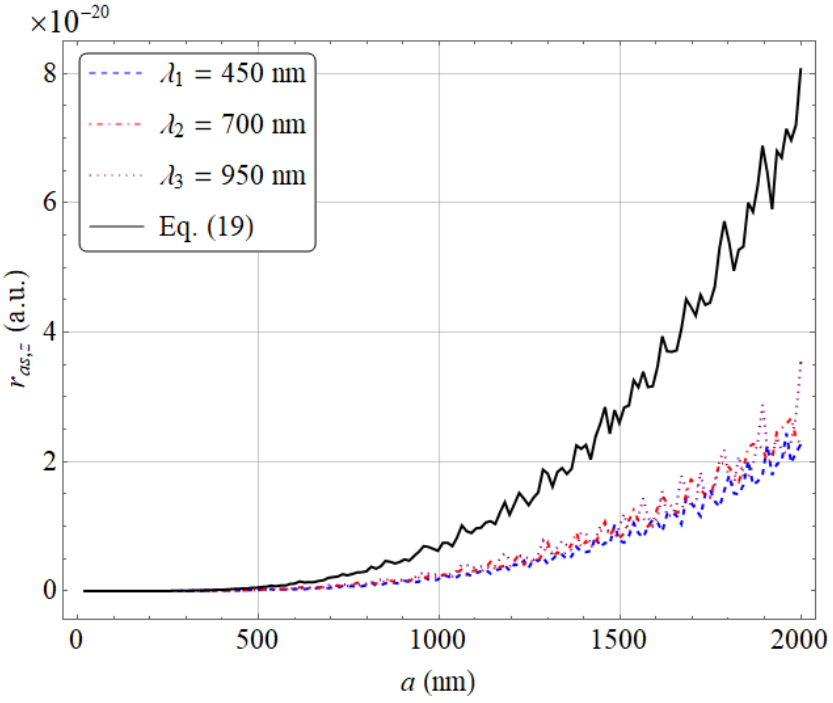

Figure 1. $r_{as,z}$ as a function of a for a multichromatic light field of wavelengths $\lambda_1 = 450$ nm, $\lambda_2 = 700$ nm and $\lambda_3 = 950$ nm. The particle is made of polystyrene, with $M_1 = 1.640 - i2.205 \times 10^{-3}$, $M_2 = 1.588 - i3.453 \times 10^{-3}$ and $M_3 = 1.564 - i4.224 \times 10^{-3}$ and $E_0(\omega_j) = 1, \forall j$.

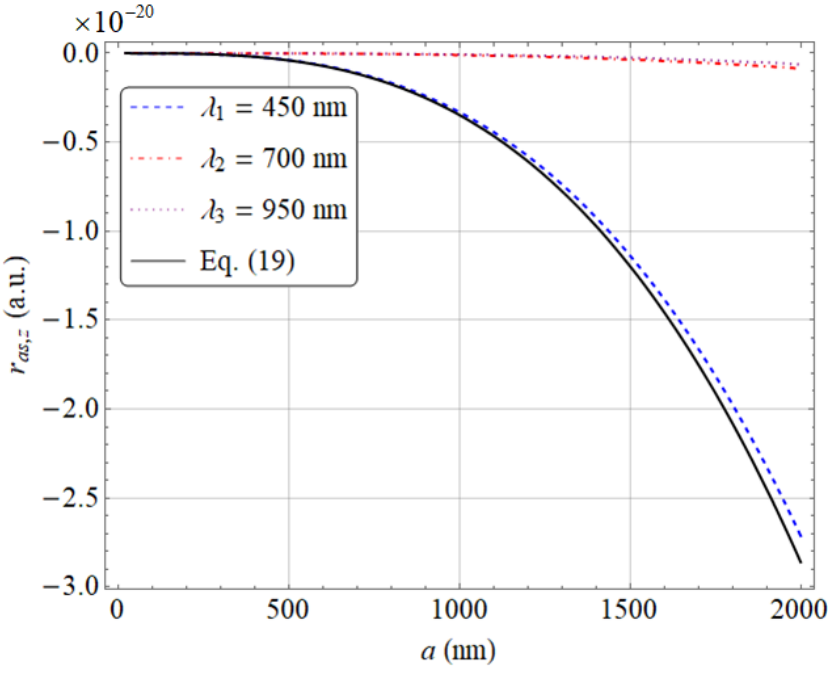

Figure 2. Same as Fig. 1, now for a gold particle with $M_1 = 1.4783 - i1.86$, $M_2 = 0.12309 - i4.1567$ and $M_3 = 0.16524 - i6.2423$.

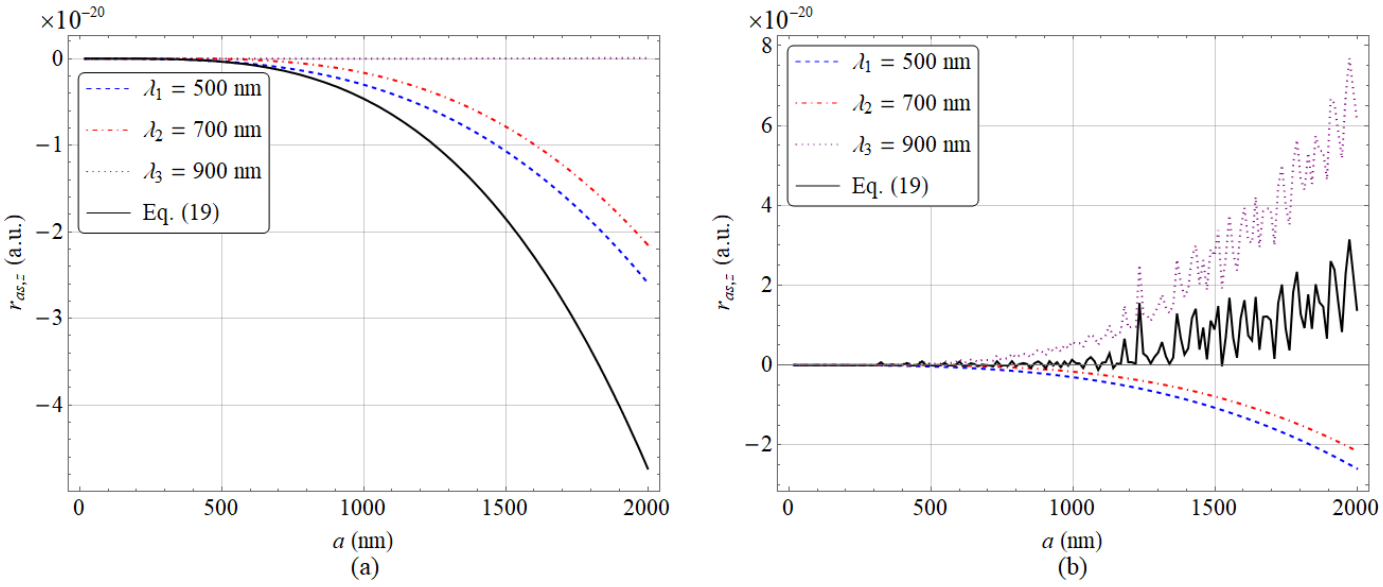

Figure 3. $r_{as,z}$ as a function of a for a multichromatic light field of wavelengths $\lambda_1 = 500$ nm, $\lambda_2 = 700$ nm and $\lambda_3 = 900$ nm. The particle is made of gallium arsenide (GaAs), with $M_1 = 4.2230 - i0.45325$, $M_2 = 3.7223 - i0.12964$ and $M_3 = 3.5325 - i1.9044 \times 10^{-4}$. (a) $E_0(\omega_1) = E_0(\omega_2) = E_0(\omega_3) = 1$. (b) $E_0(\omega_1) = E_0(\omega_2) = E_0(\omega_3)/1000 = 1$.

weighted (continuous or discrete) sum of the asymmetry factor for monochromatic plane waves, the field strengths now playing the role, in the case of a continuous dependence on angular frequency, of a spectrum. The study here proposed is still limited to uniform light and non-magnetic materials, and it would certainly be of interest to extend it in order to incorporate both arbitrary-shaped waves [by having resource, for instance, to the polychromatic generalized Lorenz-Mie theory proposed in 2022 by Ambrosio et al. (2024)] and arbitrary-index particles like negative index, magnetodielectric and other conventional or exotic materials carrying also a mag-netic response. This is currently in progress.

Funding

This work was supported by the Council for Scientific and Technological Development (CNPq) (309201/2021-7) and by the São Paulo Research Foundation (FAPESP) (2020/05280-5).

References

Ambrosio, L. A. (2020). Photophoresis in the slip-flow and free molecular regimes for arbitrary-index particles. *Journal of Quantitative Spectroscopy and Radiative Transfer*, *255*, 107276. Retrieved from https://www.sciencedirect.com/science/article/pii/S0022407320305975 doi: https://doi.org/10.1016/j.jqsrt.2020.107276

Ambrosio, L. A. (2021). Generalized Lorenz-Mie theory in the analysis of longitudinal photophoresis of arbitrary-index particles: On-axis axisymmetric beams of the first kind. *Journal of Quantitative Spectroscopy and Radiative Transfer*, *275*, 107889. Retrieved from https://www.sciencedirect.com/science/article/pii/S0022407321003812 doi: https://doi.org/10.1016/j.jqsrt.2021.107889

Ambrosio, L. A., de Sarro, J. O., & Gouesbet, G. (2024). An approach for a polychromatic generalized lorenz–mie theory. *Journal of Quantitative Spectroscopy and Radiative Transfer*, *312*, 108824. Retrieved from https://www.sciencedirect.com/science/article/pii/S0022407323003424 doi: https://doi.org/10.1016/j.jqsrt.2023.108824

Ambrosio, L. A., Wang, J., & Gouesbet, G. (2022). Towards photophoresis with the generalized Lorenz-Mie theory. *Journal of Quantitative Spectroscopy and Radiative Transfer*, *288*, 108266. Retrieved from https://www.sciencedirect.com/science/article/pii/S0022407322002011 doi: https://doi.org/10.1016/j.jqsrt.2022.108266

Arnold, S., Pluchino, A. B., & Leung, K. M. (1984, Feb). Influence of surface-mode-enhanced local fields on photophoresis. *Phys. Rev. A*, *29*, 654–660. Retrieved from https://link.aps.org/doi/10.1103/PhysRevA.29.654 doi: 10.1103/PhysRevA.29.654

Gouesbet, G., & Gréhan, G. (2017). *Generalized Lorenz-Mie Theories* (2nd ed.). Springer International Publishing.

Greene, W. M., Spjut, R. E., Bar-Ziv, E., Sarofim, A. F., & Longwell, J. P. (1985, Jun). Photophoresis of irradiated spheres: absorption centers. *J. Opt. Soc. Am. B*, *2*(6), 998–1004. Retrieved from https://opg.optica.org/josab/abstract.cfm?URI=josab-2-6-998 doi: 10.1364/JOSAB.2.000998

Mackowski, D. (1989). Photophoresis of aerosol particles in the free molecular and slip-flow regimes. *International Journal of Heat and Mass Transfer*, *32*(5), 843-854. Retrieved from https://www.sciencedirect.com/science/article/pii/0017931089902330 doi: https://doi.org/10.1016/0017-9310(89)90233-0

Magnozzi, M., Ferrera, M., Mattera, L., Canepa, M., & Bisio, F. (2018, 12). Plasmonics of Au nanoparticles in a hot thermodynamic bath. *Nanoscale*, *11*. doi: 10.1039/C8NR09038F

Papatryfonos, K., Angelova, T., Brimont, A., Reid, B., Guldin, S., Smith, P. R., ... Selviah, D. R. (2021, 02). Refractive indices of MBE-grown AlxGa(1-x)As ternary alloys in the transparent wavelength region. *AIP Advances*, *11*(2), 025327. Retrieved from https://doi.org/10.1063/5.0039631 doi: 10.1063/5.0039631

Velazco-Roa, M. A., & Thennadil, S. N. (2007, Dec). Estimation of optical constants from multiple-scattered light using approximations for single particle scattering characteristics. *Appl. Opt.*, *46*(35), 8453–8460. Retrieved from https://opg.optica.org/ao/abstract.cfm?URI=ao-46-35-8453 doi: 10.1364/AO.46.008453

Yalamov, Y., Kutukov, V., & Shchukin, E. (1976). Theory of the photophoretic motion of the large-size volatile aerosol particle. *Journal of Colloid and Interface Science*, *57*(3), 564-571. Retrieved from https://www.sciencedirect.com/science/article/pii/0021979776902344 doi: https://doi.org/10.1016/0021-9797(76)90234-4